



## OPEN Comparative analysis of stereotactic aspiration via supraorbital keyhole versus Kocher's point for basal ganglia intracerebral hematoma: computational simulation and propensity score-matched study

Jang Hun Kim<sup>1,7</sup>, Kyungwon Park<sup>2,7</sup>, Yong Hun Jung<sup>2</sup>, Sung-woo Lee<sup>1</sup>, Dong-Hyuk Park<sup>1</sup>, Sung Bom Pyun<sup>3</sup>, Joo Won Kang<sup>4</sup>, Seok Chung<sup>2,5,6</sup>✉ & Kyung-Jae Park<sup>1</sup>✉

Catheter placement via the supraorbital keyhole (SOK) for removing spontaneous intracerebral hemorrhage (sICH) in the basal ganglia may result in improved aspiration rates and functional outcomes than those by the conventional Kocher's point (KP) route. Verification was performed using the results of computational simulations and retrospective clinical data matched by propensity scores. We retrospectively enrolled 50 patients who underwent stereotactic hematoma aspiration of 'typical' shape of basal ganglia sICH. After propensity score matching (PSM), comparative analyses between the two groups ( $n = 36$ ) were performed. A computational simulation of hematoma aspiration was conducted in eight patients using 2-mm thin-sliced brain computed tomography images obtained preoperatively. After PSM, eighteen patients in each group were newly matched and the logit propensity score of the was  $0.04 \pm 0.0726$ . The aspiration rate was significantly higher in the SOK group ( $31.841 \pm 40.131$  in KP vs.  $55.191 \pm 25.387$  in SOK,  $p = 0.045$ ), and the proportion of patients who achieved good functional outcomes (mRS score, 0–2 at 6 months) was significantly higher in the SOK group (27.8% vs. 61.1%,  $p = 0.044$ ). The computational simulations also demonstrated a lower residual volume rate in the SOK group than in the KP group in those with a typical ICH type (21.5% vs. 43.4%). Stereotactic hematoma aspiration via the SOK route in patients with typical basal ganglia ICH is a safe and effective method with an enhanced aspiration rate and favorable functional outcomes.

**Keywords** Basal ganglia, Kocher's point, Spontaneous intracerebral hematoma, Stereotactic aspiration, Supraorbital keyhole

Spontaneous intracerebral hemorrhage (sICH) is the most common subtype of hemorrhagic stroke and is a critical disease, with only 12–39% of survivors achieving long-term functional independence<sup>1</sup>. Recent studies have demonstrated that the basal ganglia region exhibits the highest incidence of sICH. Its location often correlates with decreased levels of consciousness and motor deficits in patients with contralateral hemiplegia<sup>2</sup>. To reduce secondary injury caused by the physiological response of the hematoma, such as perilesional edema

<sup>1</sup>Department of Neurosurgery, Korea University Anam Hospital, Korea University College of Medicine, Seoul, Korea. <sup>2</sup>School of Mechanical Engineering, Korea University, Seoul, Korea. <sup>3</sup>Department of Rehabilitation Medicine, Korea University Anam Hospital, Korea University College of Medicine, Seoul, Korea. <sup>4</sup>Department of Neuroscience, University of Illinois Chicago, Chicago, IL, USA. <sup>5</sup>KU-KIST Graduate School of Converging Science and Technology, Korea University, Seoul, Korea. <sup>6</sup>Center for Brain Technology, Brain Science Institute, Korea Institute of Science and Technology, Seoul, Korea. <sup>7</sup>These authors contributed equally: Jang Hun Kim and Kyungwon Park (as co-first author). ✉email: sidchung@korea.ac.kr; kyungjae99@hanmail.net

and inflammatory reactions from blood product toxicity<sup>3</sup>, surgical intervention for hematoma evacuation is often necessary to eliminate neurotoxic metabolites and reduce the mass effect of the hematoma<sup>4–7</sup>.

Unfortunately, several large randomized controlled trials (RCTs) have failed to demonstrate significant improvements in overall functional outcomes for surgical treatment compared to best medical care in basal ganglia intracerebral hemorrhage (ICH)<sup>4,8–10</sup>. This highlights the complexity of managing these cases and the need for careful patient selection. Recent clinical trials, however, have explored minimally invasive techniques for hematoma evacuation, offering some promising results. The MISTIE series demonstrated that minimally invasive surgery plus recombinant tissue plasminogen activator (rtPA) showed greater clot resolution than traditional medical management. The ICES trial described intraoperative CT-guided endoscopic surgery as safe and effective for removing acute intracerebral hematomas, with the potential to enhance neurological recovery. Most recently, the ENRICH trial presented that minimally invasive hematoma evacuation resulted in better functional outcomes at 180 days than guideline-based medical management in patients with lobar or anterior basal ganglia ICHs<sup>11</sup>.

However, the details of location-tailored surgical techniques, such as safe entry points, target trajectories, appropriate aspiration pressures, catheter diameters, and postoperative alteplase protocols, have not yet been fully established. In clinical settings, the Kocher's point (KP) approach is widely used for inserting a catheter in patients with basal ganglia sICH owing to its established safety, feasibility, and accuracy, as supported by previous retrospective studies<sup>4,8–10,12–14</sup>. The KP approach was originally devised for ventriculostomy, which targets the foramen Monro of the lateral ventricle starting from the middle frontal gyrus<sup>15</sup>. Owing to the anatomical proximity between the lateral ventricle and basal ganglia, the KP approach has become the preferred method for performing stereotactic hematoma aspiration procedures for sICH located in the lentiform nucleus of the globus pallidus or putamen. Recently, supraorbital keyhole (SOK) surgeries using the anterior skull base approach have been widely used in the treatment of tumors or neurovascular diseases. Ventriculostomy via the basal frontal lobe has been attempted using the SOK approach, which demonstrated acceptable safety and feasibility<sup>16–18</sup>.

Anatomically, the lentiform nucleus of the basal ganglia has an average length (anterior-to-posterior (AP)) of approximately 41–47 mm, which is far longer than its height (superior-to-inferior (SI), approximately 20 mm)<sup>19</sup>. We hypothesized that positioning a catheter with a longer diameter in the AP direction (SOK approach) would enable it to come in contact with the widest area of a typical hematoma, potentially resulting in a higher aspiration rate than that resulting by placing a catheter in the S-I direction (KP approach) (Fig. 1). Since other types of hematoma aspiration surgeries (tubular or endoscopic hematoma aspirations) frequently accompany the parenchyma injury along the trajectories, this long-axis concept was understood as an important tactic in these kinds of surgeries<sup>20</sup>. To verify this hypothesis, we conducted: (1) A retrospective analysis of clinical

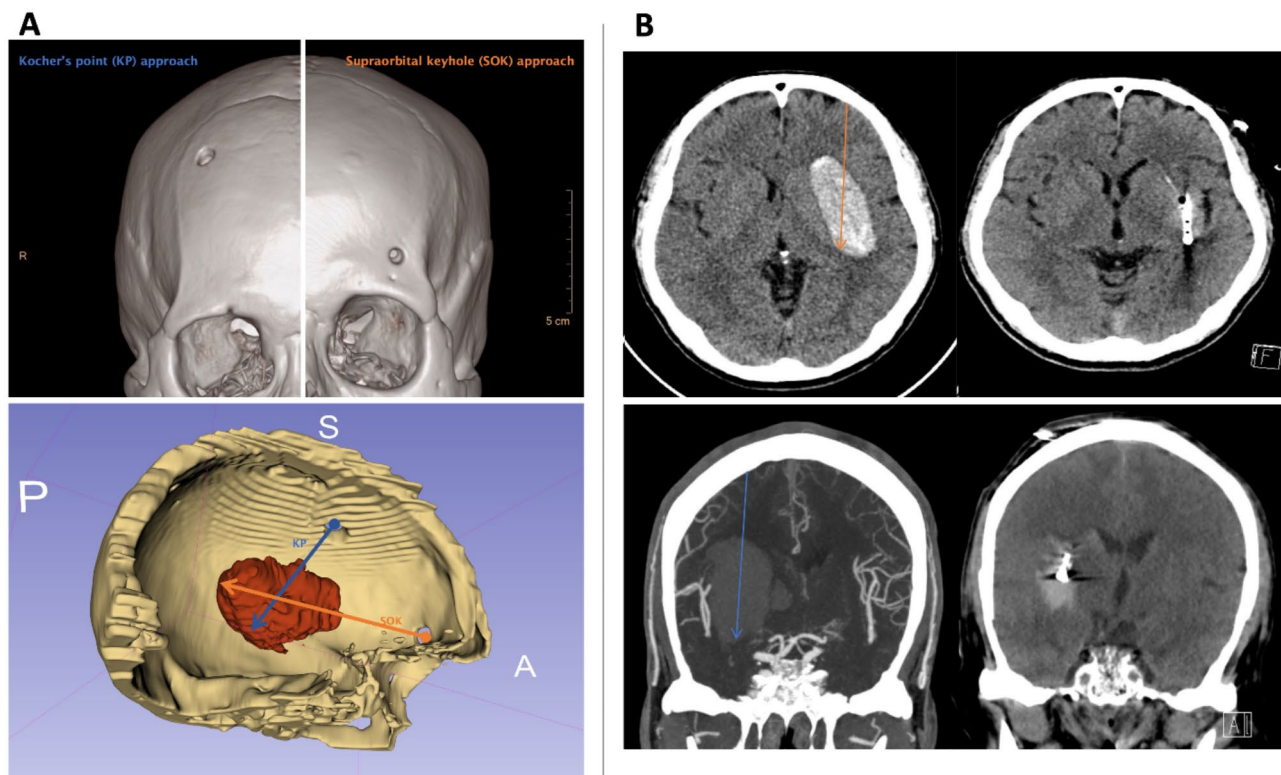


**Fig. 1.** Two trajectories for accessing the basal ganglia sICH; (A) Burr hole sites for two entries and consequent trajectories; (B) Axial CT scans for SOK approach (upper) and coronal CT scans for KP approach (lower). Blue: Kocher's point (KP); orange: supraorbital keyhole (SOK).

data using propensity score matching (PSM) to compare outcomes between the SOK and KP approaches; (2) Computational simulations to verify the theoretical advantages of the SOK route in hematoma aspiration.

## Materials and methods

### Patients

Between January 2010 and December 2021, data of 243 patients diagnosed with sICH who underwent surgery were retrospectively reviewed. The patients were classified as (1) those diagnosed with sICH in the “basal ganglia” and (2) those who underwent frameless stereotactic hematoma aspiration surgery alone using either the SOK or KP approach. Patients with a Glasgow coma scale (GCS) score of  $\geq 5$ , a hematoma volume of  $\geq 20$  mL with neurological signs and symptoms, and no surgical contraindications including an underlying medical disease were included in the study. Meanwhile, patients with ICH caused by other factors ( $n=42$ ), those with ICH in other locations ( $n=94$ ), or those who underwent other types of surgical interventions ( $n=31$ ) were excluded. Finally, only 76 patients were selected. A flowchart of the study is shown in Fig. 2. The 76 reviewed patients were divided into the “typical” and “atypical” groups according to the shape of the hematoma. The typical type was defined when the length (A-P) of the hematoma exceeded its height (S-I) by at least 20% in a three-dimensional (3D) reconstructed image (Fig. 3). The current study was approved by the Institutional Review Board of the Human Research Center of Korea University Anam Hospital. All procedures performed in studies involving human participants were in accordance with the ethical standards of the institutional and with the 1964 Helsinki Declaration and its later amendments or comparable ethical standards. Due to retrospective nature of the study, informed consent was waived by the Institutional Review Board of the Human Research Center of Korea University Anam Hospital.

Due to retrospective nature of the study Informed consent was waived by (the name of the IRB).

The patient’s general demographic and clinical data were retrospectively gathered, including age, sex, medical history (hypertension, diabetes, dyslipidemia, and previous stroke), medication history (use of antiplatelet or

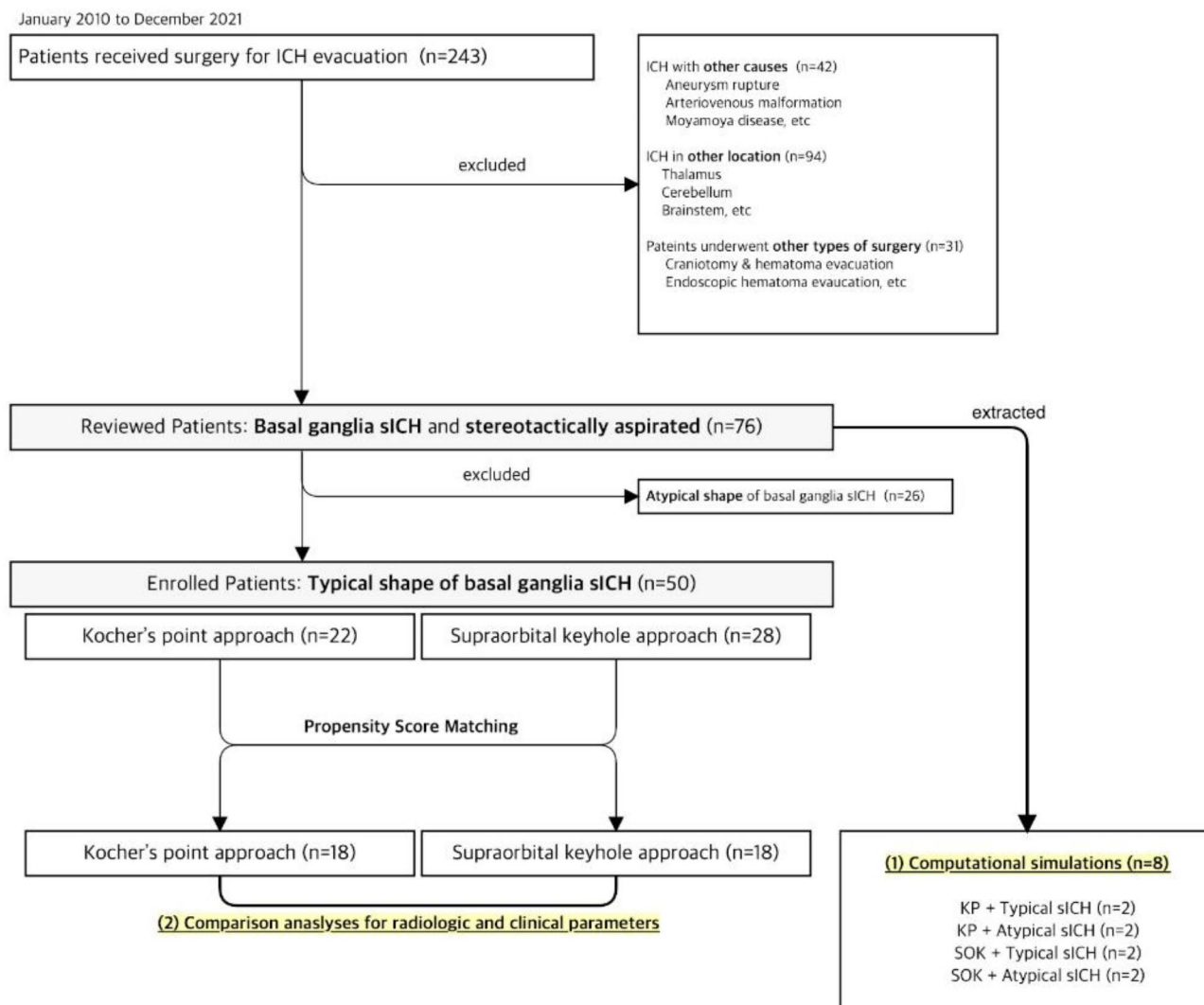


**Fig. 2.** Flow chart of the patient selection process.

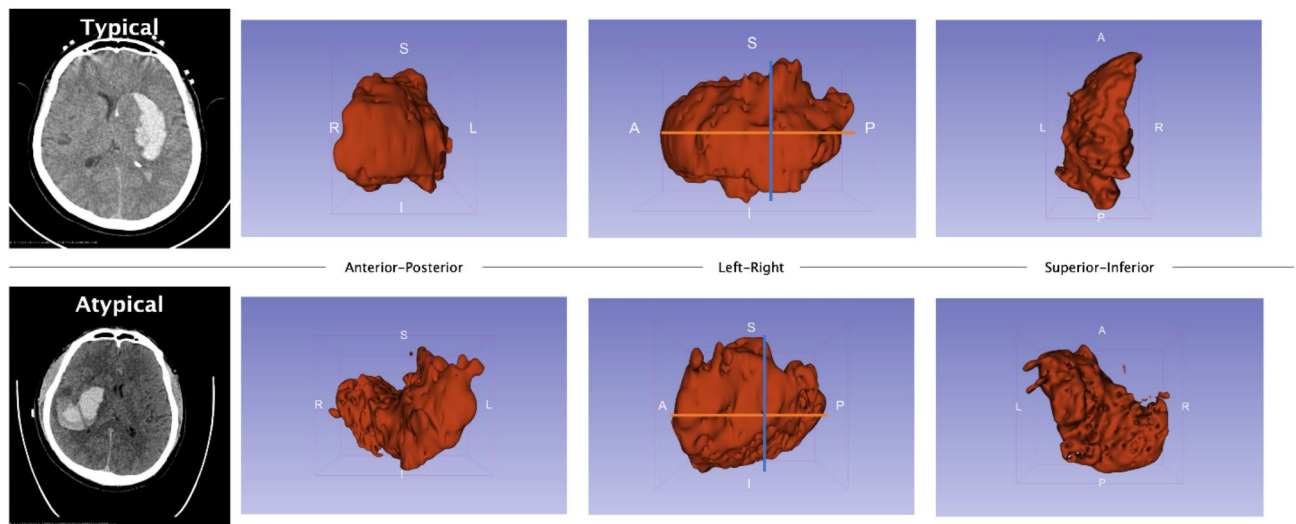


**Fig. 3.** Three-dimensional reconstructed images of sICH: Representative patients with typical (upper) and atypical (lower) hematoma shapes. Hematomas with an anterior-posterior diameter of  $>20\%$  longer than the superior-inferior diameter were defined as “typical”.

anticoagulant agents), onset to operation time, GCS score upon admission, the level of consciousness, and pupillary responses. To evaluate the outcomes, the length of intensive care unit stays, total length of hospital stays, Glasgow outcome scale scores at discharge, and modified Rankin Scale (mRS) scores at 3 and 6 months were also reviewed.

### Radiologic evaluation

The source data of preoperative 2-mm thin-sliced brain computed tomography (CT) and postoperative 5-mm thin-sliced brain CT images were acquired in the Digital Imaging and Communications in Medicine format. Only intraparenchymal hematomas were manually identified pixel by pixel in each slice, after the setting thresholds of 40–100 Hounsfield units. Hematoma segmentation modeling was performed using the free open-source software, 3D Slicer (version 4.10.2, 3D Slicer, <https://www.slicer.org>). Two physicians independently segmented the hematoma, and the median hematoma volumes were used (Supplementary Fig. 1). Using the preoperative images, the following radiologic findings were evaluated: midline shifting, the side of the involved hemisphere, the presence of intraventricular hemorrhage, the absence of a basal cistern (ipsilateral), hematoma shape, and hematoma volume. Using the postoperative images, catheter-related complications, such as poor catheter positioning, hematoma expansion, and catheter-related bleeding (axis injury), were evaluated.

### Operative technique

Prior to surgery, the stereotactic indicator was stitched to the forehead of the patient using a frameless technique. The stereotactic coordinates of the lesion were determined from a 2-mm thin-sliced brain CT scan using a neurosurgical navigation system (Stealth Station, Medtronic, Broomfield, CO, USA). Under general endotracheal anesthesia, the patient was placed in the supine position, with the head gently immobilized. The skin was carefully prepared with an aseptic betadine solution to prevent infection, followed by sterile draping. A skin incision was created either at the KP or supraorbital area. For the SOK approach, a small incision was made at the lateral half of the superior margin of the eyebrow, and a burr hole was created above the supraorbital ridge lateral to the supraorbital notch. A small dural and cortical incision was then made through bipolar cauterization, and a catheter was inserted to evacuate the hematoma following the calculated coordinates under the navigation guide. The catheter was initially inserted 5 mm into the deepest portion of the trajectory and then withdrawn. Manual aspiration with negative pressure was carefully performed during withdrawal using a 10-mL syringe. Hematoma aspiration was conducted under minimal pressure ( $<2$  mL in a syringe scale). The closed drainage system was connected to a catheter for external drainage and additional thrombolytic therapy. Thrombolytic therapy with recombinant tissue plasminogen activator (rtPA) was administered if the residual hematoma volume was more than 20 cc or 50% of the preoperative hematoma volume. A 1.0 mg/1 mL dose of rtPA with 2 cc of normal saline was injected via the catheter every 12 h. The catheter was clamped for 2 h and then released for natural drainage. After surgery, neurological complications such as supraorbital neuralgia or brow ptosis were evaluated based on clinical findings.

### PSM and statistical analysis

After patient enrollment and classification into the KP ( $n=28$ ) and SOK ( $n=22$ ) groups, logistic regression analysis was conducted to estimate the correlation of each variable with the selected treatment. The coefficient estimates from this regression were subsequently used to retrospectively calculate the predicted probability (propensity score: ranging from 0 to 1) of assigning such treatment to each patient based on their characteristics.

Each patient from the SOK group was then matched with another patient (1:1 matching) from the control group based on the closest probability of treatment and size of the available control group. Once each treatment patient was matched, the unused controls were removed, and the outcomes of the SOK group were compared with those of the newly matched control group (18 SOK patients vs. 18 KP patients)<sup>21</sup>. A flowchart of the patient classification and matched classification after PSM is provided in Fig. 2.

Continuous variables were expressed as the means and standard deviations or median and interquartile ranges, while categorical variables were expressed as numbers and percentages. Independent t-tests or Mann–Whitney U tests were used for analyzing continuous variables according to the normality of distributions, while *chi-square* tests were used for analyzing categorical variables. If more than 20% of the cells in the chi-square test had an expected frequency of less than 5, the likelihood ratio or Fisher's exact test was used. A P value of < 0.05 was considered significant. Statistical analyses were performed using the standard software (version 23.0; SPSS, IBM, Chicago, IL, USA).

### 3D modeling for computational simulation

As depicted in Fig. 2, we selected eight representative patients after study enrollment and gathered their source data: four with typical sICH (two in the KP group and two in the SOK group) and four with atypical sICH (two in the KP group and two in the SOK group). Initially, the region corresponding to the hematoma was isolated from the rest by applying a threshold in the Slicer 3D program (Fig. 4A). Subsequently, the interior and exterior cavities of the hematoma were filled using the “filling holes” function to avoid unnecessary intricate surfaces and reduce simulation time (Fig. 4B). After setting the boundary conditions and removing the separate redundancies, a seamless one-body hematoma model was generated (Fig. 4C). The number of meshes was reduced using the re-mesh function in Autodesk Fusion 360 (Autodesk, Inc., San Francisco, CA, USA) while preserving the original hematoma shape and volume [Fig. 4D]. The simplified hematoma model had the same dimensions and volume as the original model. Regardless of the number of meshes (> 500), the simulation results exhibited a strong correlation.

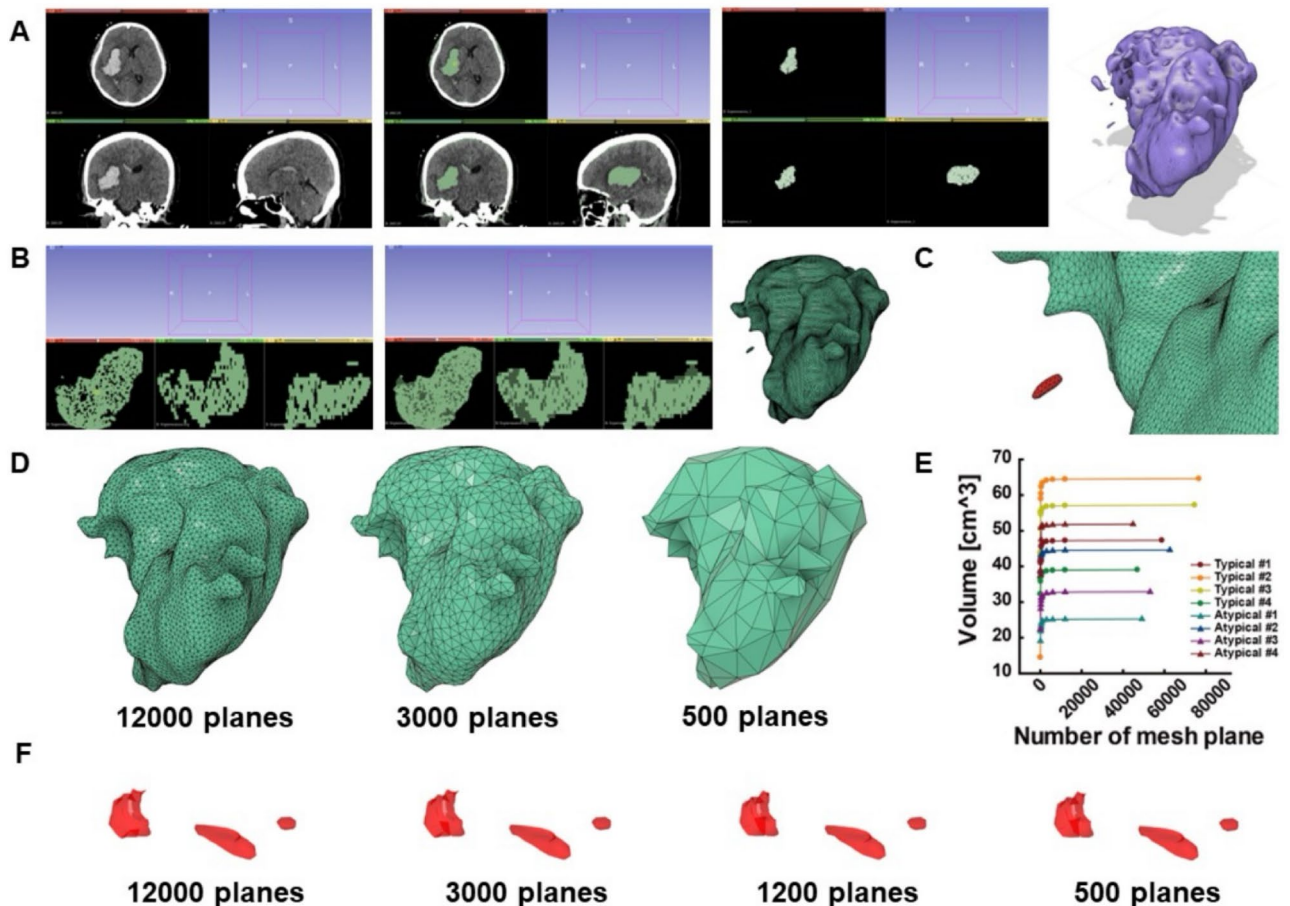


**Fig. 4.** Schematic of hematoma modeling. (A) Three-dimensional reconstruction of a thrombus from brain computed tomography data. (B) Surface simplification using the “filling holes” function of the simulator. (C) Elimination of superfluous regions. (D) Thrombus shapes with varying quantities of mesh and (E) their respective volumes. (F) Residues following suction with various mesh numbers.

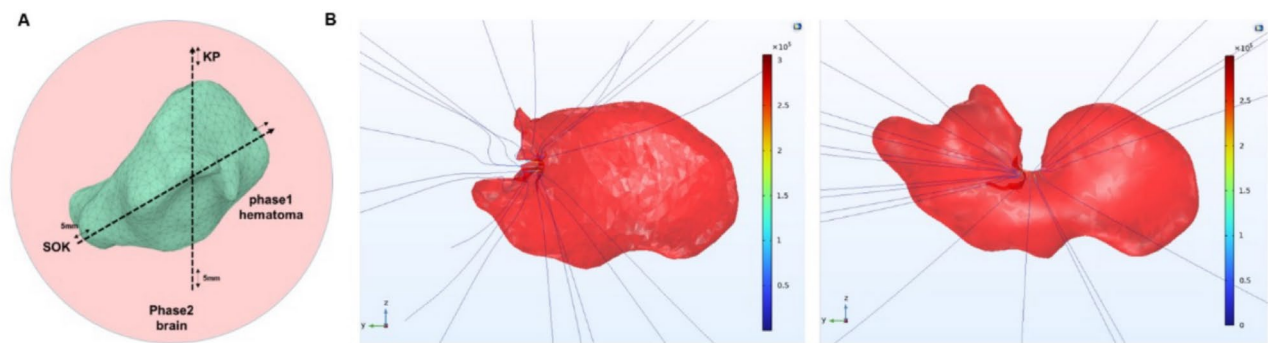


**Fig. 5.** Schematic of computational simulation. **(A)** Two catheter trajectories (SOK and KP). **(B)** Simulated hematoma changes aspirated using a catheter (left SOK, right KP). *KP* Kocher's point, *SOK* supraorbital keyhole.

$$\rho \frac{\partial \vec{V}}{\partial t} = -\nabla p + \rho \vec{g} + \mu \nabla^2 \vec{V}$$

$\mu$ Dynamic viscosity [Pa*s]	$\rho$ Density [kg/m <sup>3</sup> ]	$p$ Pressure [atm]			
Brain <sup>20</sup>	3,050	Brain <sup>21</sup>	1,050	Outlining the brain	0
Hematoma <sup>20</sup>	5,000	Hematoma <sup>21</sup>	1,300	Outlet(catheter) <sup>22</sup>	-0.8

**Table 1.** Physical values used for the simulation.

### Computational simulations

The hematoma aspiration simulation was performed using the COMSOL Multiphysics software (COMSOL, Inc., Burlington, MA, USA). The model was constructed using a two-phase solution comprising a hematoma (phase 1) and the brain (phase 2). The catheter tip had a hole with a boundary condition corresponding to the actual inner diameter of the catheter (2.5 mm) (Fig. 5). Pressure was applied to the boundary area between the circumference of the brain and catheter tip, and the Deformed Geometry function was used to simulate suction by retracting the catheter. The pressure boundary conditions were set at the boundary of the brain (Table 1). The catheter path was delineated at 5-mm intervals between the SOK or KP and the other sides of each condition. An image of the hematoma shape was generated using the isosurface function of the simulation software, and the remaining volume of the hematoma was calculated using the volume fraction function. Hematoma suction was simulated using the Navier–Stokes equation, wherein flow velocity ( $V$ ), the density of blood plasma ( $\rho$ ), pressure ( $p$ ), and viscosity ( $\mu$ ) were considered. The physical values of these variations were obtained from previous studies (Table 1).<sup>22–24</sup>

## Results

### Results of PSM

Initially, 50 patients who showed “typical basal ganglia sICH” were selected for PSM analysis, and 18 patients in each group were matched. The detailed results on PSM analysis were presented in Supplementary Fig. 4 and the logit propensity score of the matched group was  $0.04 \pm 0.0726$  with three parameters (Level of consciousness, antiplatelet usage, and initial hematoma volume).

### Results of clinical comparison analyses

The baseline demographic data of the 36 matched patients are presented in Supplementary Table 1. The patient's mean age was 55 years, while the mean hematoma volume was  $40.92 \pm 22.80$  <sup>3</sup>.

The results of the comparative analyses (KP vs. SOK) of the preoperative factors are shown in Table 2. After PSM, the preoperative factors showed no significant differences between the groups. Specifically, the preoperative hematoma volumes were  $39.41 \pm 20.11$  and  $42.42 \pm 25.71$  cm<sup>3</sup>, respectively.

The results of the main comparison analysis of the outcome parameters between the KP and SOK groups are presented in Table 3. In terms of radiologic outcomes, the incidence of catheter-related complications was lower in the SOK group ( $p=0.074$ ). In addition, a higher hematoma volume reduction was observed in the SOK group ( $13.018 \pm 14.682$  in KP vs.  $21.693 \pm 12.345$  in SOK,  $p=0.063$ ). The reduction in hematoma percentage (= aspiration rate) was significantly lower in the SOK group ( $31.841 \pm 40.131$  in KP vs.  $55.191 \pm 25.387$  in SOK,  $p=0.045$ ). In terms of clinical outcomes, the proportion of patients who achieved good functional outcomes (mRS score, 0–2 at 6 months) was significantly higher in the SOK group (27.8% vs. 61.1%,  $p=0.044$ ).

### Results of computational simulations

The results of the computational simulation of hematoma aspiration in the KP and SOK groups are depicted in Fig. 5B. Hematoma aspiration occurs in hematoma-mimicking phase 1 when negative pressure is applied

Parameters		KP (N=18)		SOK (N=18)		MD or OR	95% confidence interval		Sig.
							Lower	Upper	
<b>Patients' characteristics</b>									
Age	(Year old)	53	(37 ~ 69)	54	(32 ~ 66)	4.422	- 10.209	7.764	0.784
Sex	Female	5	(27.8%)	6	(33.3%)	1.300	0.313	5.393	0.717
Hypertension		8	(44.4%)	8	(44.4%)	1.000	0.269	3.724	1.000
Diabetes		4	(22.2%)	3	(16.7%)	0.700	0.132	3.699	0.674
Dyslipidemia		4	(22.2%)	3	(16.7%)	0.700	0.132	3.699	0.674
Prior stroke		1	(5.6%)	0	(0.0%)	0.486	0.345	0.683	0.310
Antiplatelet		1	(5.6%)	1	(5.6%)	1.000	0.058	17.325	1.000
Anticoagulant		1	(5.6%)	0	(0.0%)	0.486	0.345	0.683	0.310
<b>Neurologic status</b>									
GCS upon admission		12	(7 ~ 15)	12.5	(8.5 ~ 15)	0.954	- 2.216	1.660	0.773
	Severe	9	(50.0%)	10	(55.6%)				0.921
	Moderate	5	(27.8%)	4	(22.2%)				
	Mild	4	(22.2%)	4	(22.2%)				
Level of consciousness	Alert	2	(11.1%)	2	(11.1%)				0.355
	Drowsy	9	(50.0%)	9	(50.0%)				
	Stupor	4	(22.2%)	6	(33.3%)				
	Semi-coma	3	(16.7%)	0	(0.0%)				
	Coma	0	(0.0%)	1	(5.6%)				
Pupillary response	Equal reacting	13	(72.2%)	16	(88.9%)				0.250
	Unequal reacting	4	(22.2%)	1	(5.6%)				
	Only one reacting	1	(5.6%)	0	(0.0%)				
	Neither reacting	0	(0.0%)	1	(5.6%)				
<b>Radiologic findings</b>									
Midline shifting		5.1739	± 3.890	6.9789	± 4.573	1.41516	- 4.68094	1.07094	0.211
Side	Left	11	(61.1%)	9	(50.0%)	1.571	0.418	5.903	0.502
	Right	7	(38.9%)	9	(50.0%)				
IVH		8	(44.4%)	7	(38.9%)	0.795	0.211	3.000	0.735
Basal cistern compression		5	(27.8%)	4	(22.2%)	0.743	0.163	3.383	0.700
Volume (preoperative)	(cm <sup>3</sup> )	39.4156	± 20.112	42.4211	± 25.711	7.69409	- 18.64183	12.63072	0.699
<b>Operation findings</b>									
OP timing	Within 4 h	8	(44.4%)	7	(38.9%)				0.593
	Within 8 h	5	(27.8%)	3	(16.7%)				
	Within 24 h	5	(27.8%)	7	(38.9%)				
	After 24 h	0	(0.0%)	1	(5.6%)				

**Table 2.** Results of the comparative analyses between the KP and SOK groups: preoperative factors. *KP* Kocher's point, *SOK* supraorbital keyhole, *MD* mean difference, *OR* odds ratio, *GCS* Glasgow coma scale, *IVH* intraventricular hemorrhage.

to a catheter moving along a defined path (Fig. 6A). To simplify the simulation, a re-meshing operation was implemented to reduce the number of meshes and ultimately reduce computation time (Fig. 6B,C). To determine the maximum mesh size (minimum mesh number) required to sustain the hematoma structure and volume, the residual volume of the hematoma after suction was compared by adjusting the number of meshes (Fig. 6D). When the volumes of hematoma from eight patients were compared with the different numbers of meshes, a significant change was observed in the residual volume of patients with less than 400 meshes (Fig. 4E and F). Simulations were conducted using the actual hematoma data from eight patients divided into the typical (four patients) and atypical (four patients) groups. The simulation results demonstrate the suction value along the SOK path, particularly in patients with typical ICH. On the SOK path, the average residual volume after aspiration was 21.5%, which was significantly less than the average residual volume (43.4%) along the KP path (Fig. 6E,F). Supplementary Figs. 2 and 3 present the simulation outcomes of additional patients not shown in the main figure. A video of each simulation is also supplied in Supplementary Movies 1 and 2.

## Discussion

The current study demonstrated that stereotactic hematoma aspiration via the SOK route is a safe and effective method for patients with basal ganglia ICH, especially in those with typical hematoma shapes. Computational

Parameters		KP (N=18)		SOK (N=18)		MD or OR	95% confidence interval		Sig.
							Lower	Upper	
<b>Radiologic outcomes</b>									
Axis injury		1	(5.6%)	1	(5.6%)	1.000	0.058	17.325	1.000
Catheter-related complication	None	12	(66.7%)	17	(94.4%)				0.074 <sup>†</sup>
	Poor position	4	(22.2%)	0	(0.0%)				
	Hematoma expansion	2	(11.1%)	1	(5.6%)				
Volume (postop)	(cm <sup>3</sup> )	26.398	± 16.807	20.728	± 19.320	6.03571	- 6.59660	17.93549	0.354
Decreased hematoma volume	(cm <sup>3</sup> )	13.018	± 14.682	21.693	± 12.345	4.521341	- 17.863471	0.513471	0.063 <sup>†</sup>
Decreased volume percentage	(%)	31.841	± 40.131	55.191	± 25.387	11.192640	- 46.095346	- 0.602983	0.045*
<b>Clinical outcomes</b>									
ICU stay	(days)	12.5	(4.5 ~ 20.5)	13.50	(1.5 ~ 27.5)	4.463	- 11.070	7.070	0.657
Hospital stay	(days)	54	(28 ~ 80)	41	(12 ~ 70)	6.043	- 3.725	20.836	0.166
GOS at discharge		3	(2 ~ 4)	3.5	(2.5 ~ 4.5)	0.296	- 0.545	0.656	0.852
	1	0	(0.0%)	1	(5.6%)				0.726
	2	0	(0.0%)	0	(0.0%)				
	3	10	(55.6%)	8	(44.4%)				
	4	5	(27.8%)	6	(33.3%)				
	5	3	(16.7%)	3	(16.7%)				
mRS (3 months)		3	(2 ~ 4)	2.5	(1.5 ~ 3.5)	0.424	- 0.139	1.583	0.097 <sup>†</sup>
	0, 1	2	(11.1%)	6	(33.3%)				0.255
	2	2	(11.1%)	3	(16.7%)				
	3	7	(38.9%)	6	(33.3%)				
	4	5	(27.8%)	2	(11.1%)				
	5	2	(11.1%)	0	(0.0%)				
mRS (6 months)		3	(2 ~ 4)	2	(0 ~ 4)	0.403	- 0.264	1.375	0.177
	0, 1	2	(11.1%)	6	(33.3%)				0.250
	2	3	(16.7%)	5	(27.8%)				
	3	9	(50.0%)	4	(22.2%)				
	4	3	(16.7%)	2	(11.1%)				
	5	1	(5.6%)	0	(0.0%)				
Good functional outcome (6 months)	mRS: 0-2	5	(27.8%)	11	(61.1%)	4.086	1.007	16.579	0.044*
	mRS: 3-6	13	(72.2%)	7	(38.9%)				

**Table 3.** Results of comparative analyses between the KP and SOK groups: outcome parameters. *KP* Kocher's point, *SOK* supraorbital keyhole, *MD* mean difference, *OR* odds ratio, *ICU* intensive care unit, *GOS* Glasgow outcome scale, *mRS*, modified Rankin Scale. <sup>†</sup> $p < 0.1$ . \* $p < 0.05$ .

simulation demonstrated a higher aspiration rate using the SOK route, and comparison analysis results revealed improved radiological and clinical outcomes in the SOK group.

Various studies have explored the advantages of open hematoma evacuation compared with those of medical treatment in patients with sICH<sup>12-14,25</sup>; however, serial RCTs revealed that early surgery had no overall benefits or had minimal relative advantages on hematomas in superficial locations<sup>26,27</sup>. Instead, several studies regarding minimally invasive surgery using frameless stereotactic hematoma aspiration techniques combined with thrombolytic therapy have been performed in patients with sICH and have revealed positive results. The MISTIE I trial revealed that minimally invasive surgery plus rtPA showed greater clot resolution than traditional medical management. Moreover, rtPA does not seem to exacerbate perilesional edema<sup>4</sup>. The MISTIE II trial showed that minimally invasive surgery plus rtPA appears safe with better functional outcomes at 180 days<sup>8</sup>. The ICES trial also described intraoperative CT-guided endoscopic surgery as a safe and effective method for removing acute intracerebral hematomas, with the potential to enhance neurological recovery<sup>10</sup>. A recent meta-analysis suggested the superiority of a minimally invasive strategy over conventional craniotomy, with a lower rate of rebleeding and a higher rate of good recovery<sup>28</sup>. Although the MISTIE III trial did not show demonstrate significant improvements in the proportion of patients achieving a good long-term response within 365 days after the occurrence of moderate to large ICH<sup>9</sup>, early and rapid hematoma evacuation “theoretically” improves cerebral perfusion, eliminates blood toxic products, minimizes oxidative stresses, and ultimately leads to better functional outcomes<sup>29,30</sup>. As most previous RCTs commonly presented the safety of the procedures<sup>4,8-10</sup>, it is now widely performed in most centers in selective patients with sICH.

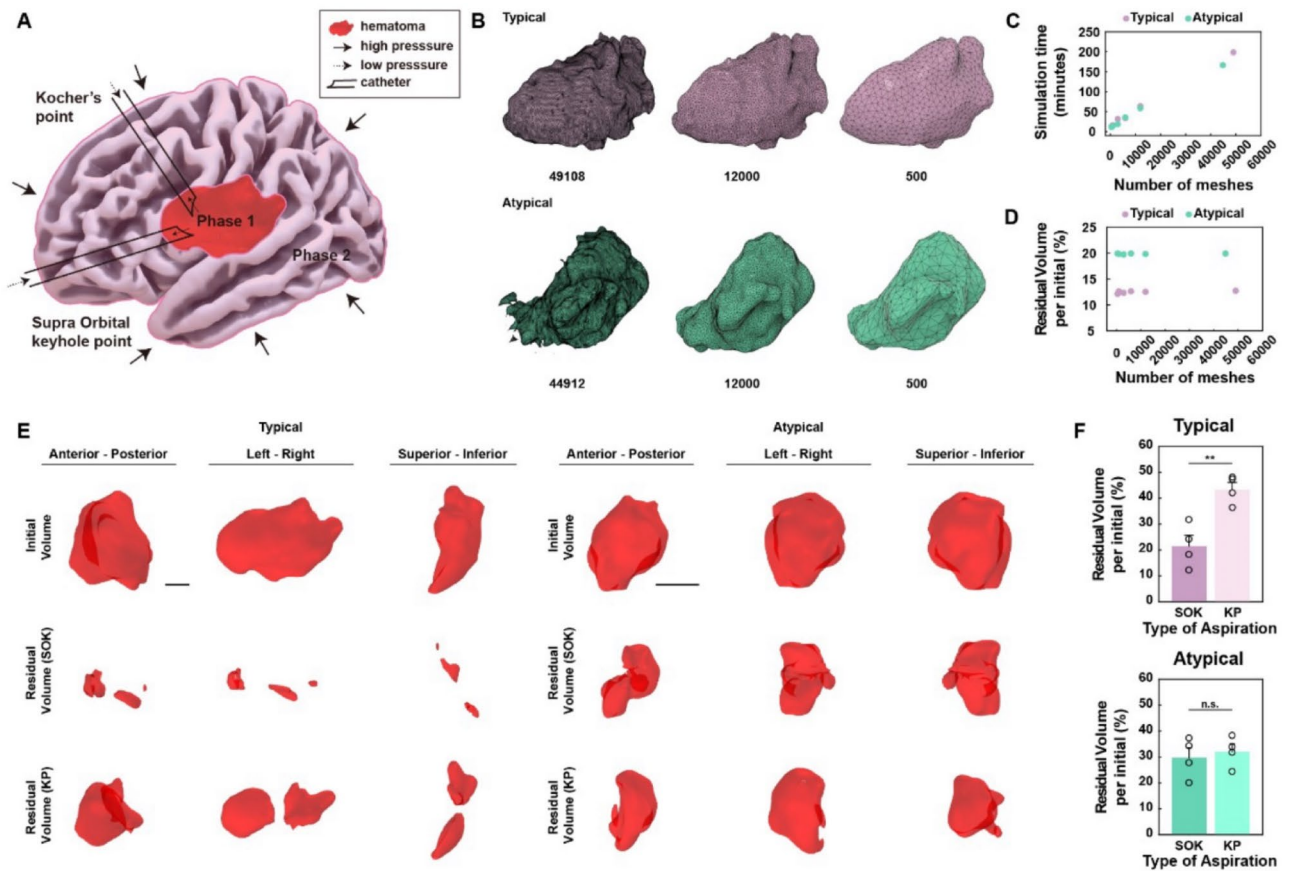


**Fig. 6.** Results of computational simulation. (A) Schematic of computational hematoma aspiration analysis. (B) The morphology of the hematoma model, both typical and atypical, dependent on the mesh numbers. (C) Simulation time required based on the mesh numbers. (D) Residual volumes of hematoma after aspiration based on the mesh numbers. (E) 3D morphologies of residual hematoma after aspiration along one of the KP or SOK paths. (F) Quantified volumes of the residual hematoma. 3D three-dimensional, KP Kocher's point, SOK supraorbital keyhole.

In cases for minimally invasive surgery, the KP route is widely used for accessing the lateral ventricle or neighboring deep brain regions (basal ganglia or thalamus) owing to its guaranteed safety and convenience (familiarity with surgeons). To the best of our knowledge, most centers use the KP route as a routine trajectory for accessing basal ganglia sICH without considering the natural shape and anatomy of the basal ganglia. With the increasing adoption of minimally invasive surgeries for accessing the anterior skull base through SOK craniotomy, growing evidence supports the safety and feasibility of accessing the lateral ventricle through the basal frontal lobe<sup>16–18</sup>. We hypothesize that the SOK route is a safe and effective alternative for sICH evacuation, considering the AP-elongated shape of the basal ganglia<sup>19</sup>.

While there have been studies exploring the use of SOK approaches for various intracranial procedures, research specifically focusing on hematoma removal in basal ganglia sICH via this route is limited. It's important to note that our study is unique in its specific enrollment of patients with deep-seated basal ganglia hematoma. For instance, Oh et al. (2022) investigated supraorbital endoscopic evacuation in patients with frontal traumatic ICH, which primarily involved subcortical hematomas<sup>31</sup>. This patient population differs significantly from our focus on deep-seated basal ganglia ICH. Similarly, Zheng et al. (2024) examined the utility of the supraorbital eyebrow arch keyhole approach for various skull base procedures, but did not specifically address catheter insertion for basal ganglia hematoma evacuation<sup>32</sup>. Our study, therefore, addresses a gap in the literature by specifically evaluating the efficacy of the supraorbital keyhole approach for stereotactic aspiration of typical basal ganglia ICH.

In terms of safety, eyebrow incision-related complications such as brow ptosis (associated with facial nerve injury) or frontal neuralgia (associated with supraorbital nerve injury) did not occur. This low incidence of complications is attributed to the small incision (2 cm) created on the lateral supraciliary line during a small burr hole craniotomy, which avoids the dangerous anatomy of the facial or supraorbital nerve (Fig. 1A). Furthermore, no significant differences were observed in the incidence of catheter-related complications between the SOK approach and the KP approach<sup>33</sup>. Every aspect of the procedure mirrored that of the KP approach, except for a slightly deeper engagement of the catheter by 1–2 cm through the white matter. Importantly, this difference did not affect the significant complication rate. When focusing on the AP-elongated ellipsoid type of hematoma,

the total length from the bone margin to the hematoma is relatively the same in both approaches (Fig. 1B). Compared with traditional KP, the SOK approach enables a longer trajectory within the hematoma. This approach enables hematoma evacuation with just a single pass of the catheter, thus minimizing iatrogenic brain injury. This trajectory provides a multifocal aspiration core with only a single tract by reciprocating motion<sup>34</sup>. Moreover, considering the cerebral superficial venous system, the SOK approach has a lower likelihood of encountering midline superficial cortical veins compared with the KP approach<sup>35</sup>. Thus, the risk of postoperative venous infarction can be avoided.

In terms of efficacy, the aspiration rate achieved using the SOK approach was notably higher when the cohorts were compared. Specifically, the subgroup analysis revealed significantly improved radiological (aspiration rate) and clinical (favorable mRS score) outcomes in the SOK group, suggesting that patients with typical basal ganglia sICH may be suitable for the supraorbital approach. Our results indicate that 50 of 76 (65.8%) patients showed a typical AP-elongated ellipsoid pattern, allowing for the insertion of a catheter with a longer diameter via the SOK route. This suggests that the majority of patients with basal ganglia sICH can be assessed using the simple eyebrow approach. Although the efficacy of the SOK route was sufficiently verified using clinical data, it has inherent limitations, including its retrospective design; small sample size; and biases such as surgeon preference, patient selection, and differences in baseline characteristics. To address these limitations, we conducted a computational simulation to establish foundational qualifications and provide academic verification.

Computational simulations confirmed that aspiration via the SOK route generated less residual hematoma in patients with typical ICH. Further simulations using an imaginary simple oval hematoma revealed the formation of a large notch when the aspiration catheter moved vertically along the shorter axis (Supplementary Fig. 5). Notches were also observed around the horizontally inserted non-moving catheters. Under negative pressure, the interfacial tension at the boundary surface of the hematoma near the entrance of the catheter caused the formation of notches. When the catheter remained stationary, two notches were formed on the upper and lower planes of the hematoma surface, closer to the catheter entrance. In dynamic simulations that account for catheter movement, the starting point of catheter motion was close to the hematoma surface when the catheter was vertically pulled out. As the catheter moved, a small notch initially formed on the hematoma surface plane parallel to and near the catheter entrance, which subsequently grew in size (Supplementary Movie 3). The developed notch disrupts the aspirated flow of hematoma, thereby increasing the likelihood of flow disruption and residue formation. In the simulation, the advantage of the SOK route in the typical group can be attributed to the (i) reduced movement at the hematoma surface parallel (orange) and close to the catheter entrance at the beginning, (ii) reduced distance between the hematoma surface planes (green) to the catheter entrance during catheter movement, and (iii) increased total stroke along the long axis of the hematoma. The distances from the catheter entrance to the parallel (orange) or normal planes (green) are shown [Supplementary Fig. 5C,D].

Simulations under two-phase flow conditions can predict both the volume and morphology of the residual hematoma after aspiration. To avoid sharp edges between meshes, phase 1 (hematoma) must be attached inside phase 2 (brain) under such large deformation conditions (Supplementary Fig. 6). During a rapid change in hematoma volume, meshes in the single-phase simulation move only under the constraints of neighboring meshes and form unbound acute angles. There was an error regardless of the mesh size. The catheter speed and aspiration pressure can be adjusted by clinicians. In our simulation, the negative pressure generated by a 10-cc syringe was calculated assuming that the piston was fully retracted. In actual clinical treatment, the catheter moves back and forth multiple times; during our simulation, the catheter moved in a single stroke. Using individual CT data and personal computers, the simulation was completed within a few hours. The developed method can calculate the residual hematoma after aspiration along a specific path, along with the size and morphology of each hematoma. This approach enables physicians to estimate the efficacy of moving a catheter along a specific aspiration path during the treatment of typical ICH.

## Conclusions

The current study demonstrated that stereotactic hematoma aspiration via the SOK route is safe and effective in patients with basal ganglia ICH. Notably, patients with the typical shape of ICH demonstrated a significantly improved aspiration rate and more favorable outcomes. To overcome the limitations of a retrospective analysis, we compared these two routes using a computational simulation of hematoma aspiration. The findings from our simulation revealed a superior aspiration rate via the SOK route in patients with typical basal ganglia ICH.

## Data availability

Data supporting the findings of this study are not publicly available. The data are available from the authors upon reasonable request and with the permission of the corresponding author.

Received: 25 September 2024; Accepted: 3 March 2025

Published online: 05 April 2025

## References

1. An, S. J., Kim, T. J. & Yoon, B. W. Epidemiology, risk factors, and clinical features of intracerebral hemorrhage: an update. *J. Stroke* **19** (1), 3–10. <https://doi.org/10.5853/jos.2016.00864> (2017).
2. Wang, S. et al. Epidemiology of intracerebral hemorrhage: A systematic review and meta-analysis. *Front. Neurol.* **13**, 915813. <https://doi.org/10.3389/fneur.2022.915813> (2022).
3. Aronowski, J. & Zhao, X. Molecular pathophysiology of cerebral hemorrhage: secondary brain injury. *Stroke* **42** (6), 1781–1786. <https://doi.org/10.1161/STROKEAHA.110.596718> (2011).
4. Mould, W. A. et al. Minimally invasive surgery plus Recombinant tissue-type plasminogen activator for intracerebral hemorrhage evacuation decreases perihematomal edema. *Stroke* **44** (3), 627–634. <https://doi.org/10.1161/STROKEAHA.111.000411> (2013).

5. Gebel, J. M. Jr. et al. Natural history of perihematomal edema in patients with hyperacute spontaneous intracerebral hemorrhage. *Stroke* **33** (11), 2631–2635. <https://doi.org/10.1161/01.str.0000035284.12699.84> (2002).
6. Chen, X. et al. The impact of intracerebral hemorrhage on the progression of white matter hyperintensity. *Front. Hum. Neurosci.* **12**, 471. <https://doi.org/10.3389/fnhum.2018.00471> (2018).
7. Ropper, A. H. Lateral displacement of the brain and level of consciousness in patients with an acute hemispherical mass. *N Engl. J. Med.* **314** (15), 953–958. <https://doi.org/10.1056/NEJM198604103141504> (1986).
8. Hanley, D. F. et al. Safety and efficacy of minimally invasive surgery plus Alteplase in intracerebral haemorrhage evacuation (MISTIE): a randomised, controlled, open-label, phase 2 trial. *Lancet Neurol.* **15** (12), 1228–1237. [https://doi.org/10.1016/S1474-4422\(16\)30234-4](https://doi.org/10.1016/S1474-4422(16)30234-4) (2016).
9. Hanley, D. F. et al. Efficacy and safety of minimally invasive surgery with thrombolysis in intracerebral haemorrhage evacuation (MISTIE III): a randomised, controlled, open-label, blinded endpoint phase 3 trial. *Lancet* **393** (10175), 1021–1032. [https://doi.org/10.1016/S0140-6736\(19\)30195-3](https://doi.org/10.1016/S0140-6736(19)30195-3) (2019).
10. Vespa, P. et al. ICES (Intraoperative stereotactic computed Tomography-Guided endoscopic Surgery) for brain hemorrhage: A multicenter randomized controlled trial. *Stroke* **47** (11), 2749–2755. <https://doi.org/10.1161/STROKEAHA.116.013837> (2016).
11. Pradilla, G. et al. Trial of early minimally invasive removal of intracerebral hemorrhage. *N Engl. J. Med.* **390** (14), 1277–1289. <https://doi.org/10.1056/NEJMoa2308440> (2024).
12. Morgan, T. et al. Preliminary findings of the minimally-invasive surgery plus RtPA for intracerebral hemorrhage evacuation (MISTIE) clinical trial. *Acta Neurochir. Suppl.* **105**, 147–151. [https://doi.org/10.1007/978-3-211-09469-3\\_30](https://doi.org/10.1007/978-3-211-09469-3_30) (2008).
13. Miller, C. M., Vespa, P. M., McArthur, D. L., Hirt, D. & Etchepare, M. Frameless stereotactic aspiration and thrombolysis of deep intracerebral hemorrhage is associated with reduced levels of extracellular cerebral glutamate and unchanged lactate pyruvate ratios. *Neurocrit Care.* **6** (1), 22–29. <https://doi.org/10.1385/NCC:6:1:22> (2007).
14. Hattori, N., Katayama, Y., Maya, Y. & Gatherer, A. Impact of stereotactic hematoma evacuation on activities of daily living during the chronic period following spontaneous putaminal hemorrhage: a randomized study. *J. Neurosurg.* **101** (3), 417–420. <https://doi.org/10.3171/jns.2004.101.3.0417> (2004).
15. Schultke, E. Theodor Kocher's craniometer. *Neurosurgery* **64** (5), 1001–1004. <https://doi.org/10.1227/01.NEU.0000344003.72056.7F> (2009). discussion 1004–1005.
16. Bhattarai, R. et al. Supraorbital eyebrow keyhole approach for microsurgical management of ruptured anterior communicating artery aneurysm. *Exp. Ther. Med.* **20** (3), 2079–2089. <https://doi.org/10.3892/etm.2020.8909> (2020).
17. Zheng, S. F., Yao, P. S., Yu, L. H. & Kang, D. Z. Keyhole approach combined with external ventricular drainage for ruptured, Poor-Grade, anterior circulation cerebral aneurysms. *Medicine* **94** (51), e2307. <https://doi.org/10.1097/MD.0000000000002307> (2015).
18. Menovsky, T., De Vries, J., Wurzer, J. A. & Grotenhuis, J. A. Intraoperative ventricular puncture during supraorbital craniotomy via an eyebrow incision. Technical note. *J. Neurosurg.* **105** (3), 485–486. <https://doi.org/10.3171/jns.2006.105.3.485> (2006).
19. Hernando, R. & Pedro, M. Surgical anatomy of the putamen. *Turkish Neurosurg.* **3** (Num 1), 11–14 (1993).
20. Chartrain, A. G. et al. A review and comparison of three neuronavigation systems for minimally invasive intracerebral hemorrhage evacuation. *J. Neurointerv. Surg.* **10** (1), 66–74. <https://doi.org/10.1136/neurintsurg-2017-013091> (2018).
21. Kane, L. T. et al. Propensity score matching: A statistical method. *Clin. Spine Surg.* **33** (3), 120–122. <https://doi.org/10.1097/BSD.0000000000000932> (2020).
22. Pennati, G., Balossino, R., Dubini, G. & Migliavacca, F. Numerical simulation of thrombus aspiration in two realistic models of catheter tips. *Artif. Organs.* **34** (4), 301–310. <https://doi.org/10.1111/j.1525-1594.2009.00770.x> (2010).
23. Nahirnyak, V. M., Yoon, S. W. & Holland, C. K. Acousto-mechanical and thermal properties of clotted blood. *J. Acoust. Soc. Am.* **119** (6), 3766–3772. <https://doi.org/10.1121/1.2201251> (2006).
24. Haseler, L. J. et al. Syringe and needle size, syringe type, vacuum generation, and needle control in aspiration procedures. *Cardiovasc. Intervent Radiol.* **34** (3), 590–600. <https://doi.org/10.1007/s00270-010-0011-z> (2011).
25. Prasad, K., Mendelow, A. D. & Gregson, B. Surgery for primary supratentorial intracerebral haemorrhage. *Cochrane Database Syst. Rev.* **4**, CD000200. <https://doi.org/10.1002/14651858.CD000200.pub2> (2008).
26. Mendelow, A. D. et al. Early surgery versus initial Conservative treatment in patients with spontaneous supratentorial intracerebral haematomas in the international surgical trial in intracerebral haemorrhage (STICH): a randomised trial. *Lancet* **365** (9457), 387–397. [https://doi.org/10.1016/S0140-6736\(05\)17826-X](https://doi.org/10.1016/S0140-6736(05)17826-X) (2005).
27. Mendelow, A. D. et al. Early surgery versus initial Conservative treatment in patients with spontaneous supratentorial Lobar intracerebral haematomas (STICH II): a randomised trial. *Lancet* **382** (9890), 397–408. [https://doi.org/10.1016/S0140-6736\(13\)60986-1](https://doi.org/10.1016/S0140-6736(13)60986-1) (2013).
28. Xia, Z. et al. Minimally invasive surgery is superior to conventional craniotomy in patients with spontaneous supratentorial intracerebral hemorrhage: a systematic review and meta-analysis. *PLoS One* **11**, e266–273. (2018).
29. Siddique, M. S. & Mendelow, A. D. Surgical treatment of intracerebral haemorrhage. *Br. Med. Bull.* **56** (2), 444–456. <https://doi.org/10.1258/0007142001903085> (2000).
30. Wilkinson, D. A. et al. Injury mechanisms in acute intracerebral hemorrhage. *Neuropharmacology* **134** (Pt B), 240–248. <https://doi.org/10.1016/j.neuropharm.2017.09.033> (2018).
31. Oh, H. J. & Hwang, S. C. Supraorbital endoscopic evacuation for traumatic intracerebral hematomas in the frontal lobe. *J. Korean Neurosurg. Soc.* **65** (6), 846–852. <https://doi.org/10.3340/jkns.2021.0248> (2022).
32. Zhou, L. et al. Clinical application of transcranial neuroendoscopy combined with supraorbital keyhole approach in minimally invasive surgery of the anterior skull base. *Sci. Rep.* **14** (1), 14886. <https://doi.org/10.1038/s41598-024-65758-y> (2024).
33. Eroglu, U. et al. Supraorbital keyhole approach: lessons learned from 106 operative cases. *World Neurosurg.* **124**, e667–e674. <https://doi.org/10.1016/j.wneu.2018.12.188> (2019).
34. Fam, M. D. et al. Surgical performance in minimally invasive surgery plus Recombinant tissue plasminogen activator for intracerebral hemorrhage evacuation phase III clinical trial. *Neurosurgery* **81** (5), 860–866. <https://doi.org/10.1093/neuros/nyx123> (2017).
35. Gardner, P. A., Engh, J., Atteberry, D. & Moossy, J. Hemorrhage rates after external ventricular drain placement. *Neurosurgery* **110** (5), 1021–1025 (2009).

## Author contributions

Two pairs of authors contributed to the research equally as co-first (J.H. Kim and K. Park) and co-corresponding authors (K-J. Park and S. Chung). J.H. Kim and K-J. Park design the study, manage the data, analyze the statistics, write manuscript and arrange the whole process of the study. K. Park, Y.H. Jung, and S. Chung manage the 3D data and simulate computationally. S-W. Lee, D.H. Park, and S.B. Pyun enrolled the patient and manage the data. J.W. Kang demonstrates the figures and conducts English correction.

## Funding

This work was supported by grants from Korea University Anam Hospital (O2207621 and O2311001), National Research Foundation of Korea (NRF) grant funded by the Korea government (MSIT)(RS-2024-00455532), and

Bio & Medical Technology Development Program of the National Research Foundation of Korea (NRF) funded by Korean government (MSIT)(RS-2024-00440577).

## Declarations

## Competing interests

The authors declare no competing interests.

## Additional information

**Supplementary Information** The online version contains supplementary material available at <https://doi.org/10.1038/s41598-025-92775-2>.

**Correspondence** and requests for materials should be addressed to S.C. or K.-J.P.

**Reprints and permissions information** is available at [www.nature.com/reprints](http://www.nature.com/reprints).

**Publisher's note** Springer Nature remains neutral with regard to jurisdictional claims in published maps and institutional affiliations.

**Open Access** This article is licensed under a Creative Commons Attribution-NonCommercial-NoDerivatives 4.0 International License, which permits any non-commercial use, sharing, distribution and reproduction in any medium or format, as long as you give appropriate credit to the original author(s) and the source, provide a link to the Creative Commons licence, and indicate if you modified the licensed material. You do not have permission under this licence to share adapted material derived from this article or parts of it. The images or other third party material in this article are included in the article's Creative Commons licence, unless indicated otherwise in a credit line to the material. If material is not included in the article's Creative Commons licence and your intended use is not permitted by statutory regulation or exceeds the permitted use, you will need to obtain permission directly from the copyright holder. To view a copy of this licence, visit <http://creativecommons.org/licenses/by-nc-nd/4.0/>.

© The Author(s) 2025